REMUNOM
ISSN 2178-6925

Received: 13/01/2026 - **Accepted:** 23/02/2026
Vol: 02.03
DOI: 10.66104/0tq2s573
Pages: 1-22

MODELAGEM E OTIMIZAÇÃO DA UNIFORMIDADE DE DISTRIBUIÇÃO DE ÁGUA EM MICROASPERSÃO VIA SUPERFÍCIE DE RESPOSTA E COMPONENTES PRINCIPAIS

MODELING AND OPTIMIZING WATER DISTRIBUTION UNIFORMITY IN MICROSPRINKLER IRRIGATION VIA RESPONSE SURFACE AND PRINCIPAL COMPONENTS

MODELADO Y OPTIMIZACIÓN DE LA UNIFORMIDAD DE DISTRIBUCIÓN DE AGUA EN MICROASPERSIÓN MEDIANTE SUPERFICIE DE RESPUESTA Y COMPONENTES PRINCIPALES

Alisson Macendo Amaral
Doutor em Ciências Agrárias - Agronomia, IFNMG – Campus Arinos, Brasil
E-mail: alisson.amaral@ifnmg.edu.br

Maria Ângela Cruz Macêdo dos Santos
Doutora em Engenharia Agrícola - Agronomia, IMA – ESEC Buritis, Brasil
E-mail: angela_macedo.08@hotmail.com

José Alberto Alves de Souza
Doutor em Engenharia Agrícola, IFBaiano – Campus Guanambi, Brasil
E-mail: alberto.souza@ifbaiano.edu.br

Alberto Luiz Ferreira Berto
Mestre em Biotecnologia, IFNMG – Campus Januária, Brasil
E-mail: alberto.berto@ifnmg.edu.br

Maria Josiane Martins
Doutora em Produção Vegetal no Semiárido, IFNMG – Campus Arinos, Brasil
E-mail: maria.martins@ifnmg.edu.br

REMUNOM
ISSN 2178-6925

Received: 13/01/2026 - **Accepted:** 23/02/2026
Vol: 02.03
DOI: 10.66104/0tq2s573
Pages: 1-22

Resumo

A eficiência da irrigação por microaspersão depende da uniformidade de distribuição de água, influenciada pela interação entre pressão de serviço e espaçamento entre emissores. Este estudo teve como objetivo modelar e otimizar o desempenho hidráulico do microaspersor Hadar 7110 por meio da integração entre Análise de Componentes Principais (PCA) e Metodologia de Superfície de Resposta (RSM). O experimento foi conduzido sob pressões variando de 0,5 a 2,5 bar e áreas por emissor entre 9 e 36 m². A PCA foi empregada para sintetizar os coeficientes de Uniformidade de Christiansen (CUC) e de Uniformidade de Distribuição (CUD) na primeira componente principal (PC1), que explicou 94.69% da variância total. Um modelo polinomial de segunda ordem foi ajustado ao PC1, apresentando bom ajuste estatístico ($R^2 = 0,8134$; $p < 0,001$). A análise canônica identificou um ponto estacionário classificado como sela, localizado em 1,46 bar e 31,15 m² por emissor, indicando ausência de ótimo interno no domínio experimental. Desempenhos superiores foram observados nas fronteiras do domínio, especialmente sob pressão próxima a 1,5 bar associada à menor área testada (9 m²). A abordagem integrada PCA–RSM demonstrou ser ferramenta robusta para harmonizar variáveis operacionais e espaciais, fornecendo suporte técnico ao dimensionamento e manejo estratégico de sistemas de microaspersão.
Palavras-chave: Engenharia de Irrigação; estatística multivariada; Hadar 7110; análise canônica.

Abstract

The efficiency of microsprinkler irrigation depends on water distribution uniformity, which is influenced by the interaction between operating pressure and spacing between emitters. This study aimed to model and optimize the hydraulic performance of the Hadar 7110 microsprinkler by integrating Principal Component Analysis (PCA) and Response Surface Methodology (RSM). The experiment was conducted under pressures ranging from 0.5 to 2.5 bar and areas per emitter between 9 and 36 m². PCA was employed to synthesize the Christiansen Uniformity Coefficient (CUC) and the Distribution Uniformity Coefficient (DU) into the first principal component (PC1), which explained 94.69% of the total variance. A second-order polynomial model was fitted to PC1, showing good statistical fit ($R^2 = 0.8134$; $p < 0.001$). Canonical analysis identified a stationary point classified as a saddle point, located at 1.46 bar and 31.15 m² per emitter, indicating the absence of an internal extremum within the experimental domain. Superior performances were observed at the domain boundaries, especially under pressure near 1.5 bar associated with the smallest area tested (9 m²). The integrated PCA–RSM approach proved to be a robust tool for harmonizing operational and spatial variables, providing technical support for the design and strategic management of microsprinkler irrigation systems.
Keywords: Irrigation Engineering; multivariate statistics; Hadar 7110; canonical analysis.

Resumen

La eficiencia del riego por microaspersión depende de la uniformidad de distribución del agua, influenciada por la interacción entre la presión de trabajo y el espaciamiento entre emisores. Este estudio tuvo como objetivo modelar y optimizar el desempeño hidráulico del microaspersor Hadar 7110 mediante la integración del Análisis de Componentes Principales (PCA) y la Metodología de Superficie de Respuesta (RSM). El experimento se llevó a cabo bajo presiones que variaron de 0,5 a 2,5 bar y áreas por emisor entre 9 e 36 m². El PCA se empleó para sintetizar los coeficientes de Uniformidad de Christiansen (CUC) y de Uniformidad de Distribución (CUD) en el primer componente principal (PC1), que explicó el 94.69% de la varianza total. Se ajustó un modelo polinomial de segundo orden al PC1, presentando un buen ajuste estadístico ($R^2 = 0,8134$; $p < 0,001$). El análisis canónico identificó un punto estacionario clasificado como punto de silla, localizado en 1,46 bar y 31,15 m² por emisor, lo que indica la ausencia de un óptimo interno en el dominio experimental. Se observaron desempeños superiores en las fronteras del dominio, especialmente bajo una presión cercana a 1,5 bar asociada a la menor área probada (9 m²). El

REMUNOM
ISSN 2178-6925

Received: 13/01/2026 - **Accepted:** 23/02/2026
Vol: 02.03
DOI: 10.66104/0tq2s573
Pages: 1-22

enfoque integrado PCA–RSM demostró ser una herramienta robusta para armonizar variables operativas y espaciales, proporcionando soporte técnico para el diseño y el manejo estratégico de sistemas de microaspersión.
Palabras clave: Ingeniería de Riego; estadística multivariada; Hadar 7110; análisis canónico.

1. Introduction

Water distribution uniformity in microsprinkler and sprinkler systems is a critical determinant of water resource use efficiency, agricultural productivity, and the sustainability of agroecosystems (Abd El-Wahed, Medici, & Lorenzini, 2016). Traditionally, the performance of these systems is measured by coefficients such as Christiansen's Uniformity Coefficient (CUC) and the Distribution Uniformity (DU), which describe the spatial variability of the applied water depth (Stambouli et al., 2023). However, analyzing these indices in isolation may be insufficient to capture hydrodynamic complexity, as performance is influenced by a synergistic interaction between operating pressure, layout geometry, and environmental factors (Chen et al. 2024; Prado et al. 2021; Rodrigues et al. 2019).

Given the multidimensional nature of these indicators, multivariate statistics—specifically Principal Component Analysis (PCA) - emerges as a robust mathematical procedure for interpreting irrigation systems. PCA allows for data dimensionality reduction, condensing the variability of multiple coefficients into a single, integrated index, commonly referred to as the first principal component (PC1). This approach minimizes statistical redundancy and provides a more representative response variable for modeling processes.

Once this integrated metric is established, Response Surface Methodology (RSM) enables the exploration of functional relationships between independent variables and the response of interest (Box & Wilson, 1951). Although well-established in industrial and chemical processes (Khuri & Cornell, 1996), the application of RSM in agricultural engineering has recently expanded to identify optimal operating regions, overcoming the limitations of conventional "one-factor-at-a-time" experimental methods (Nair; Makwana; Ahammed, 2014; Zhu et al. 2022).

The integration of PCA as a multivariate synthesis step preceding the

REMUNOM
ISSN 2178-6925

Received: 13/01/2026 - **Accepted:** 23/02/2026
Vol: 02.03
DOI: 10.66104/0tq2s573
Pages: 1-22

application of RSM remains underexplored in the hydraulic modeling of microsprinkler systems, constituting an additional methodological contribution of this study. In this sense, the objective of this work was to apply the response surface model to estimate the interdependencies between operating pressure and microsprinkler spacing on integrated uniformity (PC1). The analysis proceeded to determine and statistically classify the stationary point, establishing a quantitative basis for hydraulic optimization and the maximization of the system's operational efficiency.

2. Material and methods

The study was conducted at the Instituto Federal do Norte de Minas Gerais – Arinos Campus, in an experimental area, during the non-rainy period (July to September) at latitude 15° 55' 12.75" S, longitude 46° 8' 5.57" W, and an altitude of 525.0 m. The local climate is characterized as C2wA'a', meaning sub-humid megathermal with moderate water deficiency in winter (Oliveira and Oliveira, 2018).

A NaanDanJain microsprinkler, model Hadar 7110, was used, featuring a 1.2 mm nozzle, variable flow rate between 53 and 93 L h^{-1}, and a wetted diameter of 76.5 m at a pressure of 2 bar (manufacturer specifications). The microsprinkler pressurization system consisted of a submersible motor pump with a flow rate of 5.83 x 10^{-4} m^3 s^{-1} and a service pressure of 70 mwc (meters of water column) (6.87 bar), coupled to a 500 L reservoir. System control was performed using a ball-type shut-off valve, along with a pressure gauge to measure the pressures used in the study. The connection between the microsprinkler and the supply system was made using 16 mm diameter LDPE (Low-Density Polyethylene) hoses.

Thirty operational combinations were tested, resulting from the interaction between five service pressures (0.5 to 2.5 bar) and six spacing configurations (3x3 to 6x6 m). While pressures were measured in the field, the different spacings were obtained via computer simulation using the quadrant overlap method. After collecting volumes in 45-minute sessions and applying the proper correction for the local evaporation rate, precipitation depths (mm) were determined.

REMUNOM
ISSN 2178-6925

Received: 13/01/2026 - **Accepted:** 23/02/2026
Vol: 02.03
DOI: 10.66104/0tq2s573
Pages: 1-22

Based on these depths, the Christiansen's Uniformity Coefficient (CUC) and Distribution Uniformity (DU) were calculated (Bernardo et al., 2019). However, to capture the total variance of the system in an integrated manner, the data were subjected to Principal Component Analysis (PCA). PCA was performed in the Python environment (version 3.10), employing the PCA function from the "*scikit-learn*" library. Data were organized in a tabular structure using the "*pandas*" library and previously standardized using the StandardScaler function. Subsequently, PCA(n_components=2) was applied, considering the principal components PC1 and PC2, which together explained 100% of the total variance. Since the analysis involved two original variables, both components naturally represent the totality of the variance; however, PC1 was selected for subsequent modeling as it concentrated the highest proportion of variability and expressed the dominant direction of integrated uniformity.

This multivariate statistical procedure allowed for the dimensionality reduction of the uniformity indicators, synthesizing them into the first principal component (PC1). PC1 was adopted as the definitive response variable, representing the integrated uniformity of the system for subsequent optimization via Response Surface Methodology (RSM). The original findings up to this methodological procedure were published in Farias et al. (2024) and Amaral et al. (2025) and generated Chart 1, containing the values used in the current study for the following stages.

Chart 1 - Christiansen's Uniformity Coefficient (CUC), Distribution Uniformity (DU), and PC1 components used as modeling data. Source: Adapted from Farias et al. (2024).

Pressure (bar)	Spacing (m x m)	CUC (%)	CUD (%)	PC1
2.50	3x3	97.33	94.65	2.12
2.50	3x4	85.22	77.83	1.22
2.50	3x5	54.61	48.26	-0.82
2.50	4x4	79.06	75.67	0.93
2.50	4x6	55.47	46.70	-0.89
2.50	6x6	44.93	31.07	-1.71
2.00	3x3	95.30	95.00	1.91

REMUNOM
ISSN 2178-6925

Received: 13/01/2026 - **Accepted:** 23/02/2026
Vol: 02.03
DOI: 10.66104/0tq2s573
Pages: 1-22

2.00	3x4	87.87	81.81	1.44
2.00	3x5	63.78	61.35	-0.16
2.00	4x4	86.65	82.49	1.34
2.00	4x6	67.74	61.50	-0.09
2.00	6x6	66.91	54.92	-0.29
1.50	3x3	96.89	96.56	2.10
1.50	3x4	88.31	82.46	1.36
1.50	3x5	65.34	63.10	-0.04
1.50	4x4	88.13	83.08	1.32
1.50	4x6	68.78	60.25	-0.25
1.50	6x6	70.11	55.44	-0.50
1.00	3x3	96.16	94.91	1.94
1.00	3x4	84.35	76.52	1.08
1.00	3x5	65.48	58.07	-0.01
1.00	4x4	86.12	79.18	1.17
1.00	4x6	71.10	58.04	0.05
1.00	6x6	73.44	60.67	0.19
0.50	3x3	88.22	86.19	1.15
0.50	3x4	79.42	74.26	0.45
0.50	3x5	65.58	57.94	-0.04
0.50	4x4	81.97	39.83	-0.80
0.50	4x6	70.78	46.88	-0.76
0.50	6x6	68.08	54.06	-0.40

Although the experimental dataset was previously reported in descriptive hydraulic studies (Farias et al., 2024) and later explored using principal component analysis for treatment classification (Amaral et al., 2025), the present manuscript advances substantially beyond those approaches.

The earlier studies evaluated CUC and CUD individually or applied PCA exclusively as an exploratory multivariate classification tool. In contrast, this study integrates PCA as a dimensionality-reduction stage within a response surface modeling (RSM) framework, enabling nonlinear regression modeling, stationary point determination, and operational optimization of an integrated hydraulic performance index.

Therefore, the novelty of this work lies not in data acquisition, but in the formal statistical modeling strategy that transforms descriptive uniformity indicators

REMUNOM
ISSN 2178-6925

Received: 13/01/2026 - **Accepted:** 23/02/2026
Vol: 02.03
DOI: 10.66104/0tq2s573
Pages: 1-22

into a mathematically optimized performance surface. This modeling framework, including Hessian-based stationary point classification and model comparison procedures, was not previously implemented.

2.1 Principal Component Analysis

The linear association between Christiansen's Uniformity Coefficient (CUC) and Distribution Uniformity (CUD) was initially evaluated using Pearson's correlation coefficient. A strong and positive correlation was observed (r = 0.894), indicating substantial shared variance and statistical redundancy between the two indicators (Table 1).

Table 1 – Correlation matrix between uniformity coefficients.

	CUC	CUD
CUC	1.000	0.894
CUD	0.894	1.000

Subsequently, Principal Component Analysis (PCA) was performed on standardized variables. The eigenvalues and proportion of explained variance are presented in Table 2.

Table 2 – Eigenvalues and explained variance of principal components.

Component	Eigenvalue	Explained Variance (%)
PC1	1.959	94.69
PC2	0.110	5.31

PC1 alone explained 94.69% of the total standardized variance, demonstrating that nearly all variability contained in CUC and CUD can be represented by a single integrated component.

Table 3 – Loadings of CUC and CUD on principal components.

Variable	PC1	PC2
CUC	-0.707	0.707
CUD	-0.707	-0.707

REMUNOM
ISSN 2178-6925

Received: 13/01/2026 - **Accepted:** 23/02/2026
Vol: 02.03
DOI: 10.66104/0tq2s573
Pages: 1-22

The loadings indicate that PC1 represents a balanced linear combination of CUC and CUD, with nearly identical contributions from both variables. The negative sign reflects axis orientation and does not alter interpretation. Thus, PC1 can be expressed as:

$$PC1 = -0.707Z_{cuc} - 0.707z_{CUD}$$

or equivalently (after sign inversion),

$$PC1 = 0.707Z_{cuc} + 0.707z_{CUD}$$

The terms Z_{CUC} and Z_{CUD} represent the standardized (z-score) values of the Christiansen Uniformity Coefficient and Distribution Uniformity, respectively, obtained by centering and scaling each variable to zero mean and unit variance.

The loading value of 0.707 (≈ 1/√2) indicates that both variables contribute equally to PC1, confirming that this component represents a balanced integrated uniformity index.

Because principal component eigenvectors are defined up to sign inversion, the positive formulation was adopted for interpretative clarity.

Given that PC1 concentrates nearly all variability of the system and integrates both uniformity metrics in a statistically coherent manner, it was adopted as the response variable for subsequent Response Surface modeling.

2.2 Coding of independent variables

To ensure the statistical stability of the response surface model, the real variables (operating pressure and area per emitter) were transformed into coded variables (x1 – operating pressure and x2 – area per emitter) within the interval from -1 to +1. According to Khuri and Cornell (1996), this dimensionless standardization is fundamental to avoid multicollinearity and allow for a direct comparison between factor effects. The transformation followed Eq. 1.

$$x_i = \frac{X_i - X_{center}}{\Delta X} \quad (1)$$

REMUNOM
ISSN 2178-6925

Received: 13/01/2026 - **Accepted:** 23/02/2026
Vol: 02.03
DOI: 10.66104/0tq2s573
Pages: 1-22

Where: X_{center} is the midpoint of the experimental interval; ΔX corresponds to half the factor's range.

2.3 Response surface model fitting

To analyze the data, a second-order polynomial model was fitted, based on the classical structure of Response Surface Methodology (RSM), as presented in Eq. 2. The model was estimated by multiple linear regression using the ordinary least squares (OLS) method. The statistical significance of the coefficients was evaluated by individual t-tests (α = 0.05), while the overall quality of the fit was verified through analysis of variance (F-test) and the coefficient of determination (R^2). Additionally, residual diagnostics were performed to verify the model assumptions.

$$Y = \beta_0 + \beta_1 x_1 + \beta_2 x_2 + \beta_{11} x_1^2 + \beta_{22} x_2^2 + \beta_{12} x_1 x_2 + \varepsilon \quad (2)$$

Where: Y = estimated value for the first principal component (PC1); x_1: coded level of the operating pressure; x_2: coded level of the area per emitter; β_0: model intercept (Y value at the center point); β_1, β_2: linear regression coefficients for pressure and area, respectively; β_{11}, β_{22}: quadratic regression coefficients; β_{12} = interaction coefficient between pressure and area; ε: experimental random error assumed to have a normal distribution N (0, σ^2).

2.4 Determination and classification of the stationary point

The optimization of the response surface was performed by locating the stationary point, defined as the point where the function gradient is zero (∇Y = 0). Mathematically, the coordinates of the stationary point were obtained by solving the system of equations formed by the first-order partial derivatives with respect to the independent variables (∂Y/∂x1 = 0 and ∂Y/∂x2 = 0). The resulting linear system was solved via matrix algebra, as shown in Eq. 3:

$$X_s = -\frac{1}{2} B^{-1} b \quad (3)$$

REMUNOM
ISSN 2178-6925

Received: 13/01/2026 - **Accepted:** 23/02/2026
Vol: 02.03
DOI: 10.66104/0tq2s573
Pages: 1-22

Where: X_s = vector of stationary point coordinates in coded variables (pressure and area per emitter); *B*= symmetric matrix of second-order (quadratic) coefficients of the fitted response surface model; B^{-1}= inverse of matrix B; *b*= vector of first-order (linear) regression coefficients.

After determining the coordinates in the coded system, they were converted back to the real scale of the variables (pressure and area). The characterization of the nature of the stationary point was performed through the analysis of the Hessian matrix (H), Eq. 4:

$$H = \left[\frac{2\beta_{11}}{\beta_{12}} \frac{\beta_{12}}{2\beta_{22}}\right] \quad (4)$$

Where: H = Hessian matrix (or second-order derivative matrix); β_{11}, β_{22} = quadratic effects (quadratic regression coefficients); β_{12}= interaction coefficient between pressure and area.

2.5 Response surface visualization

The response surface was graphically represented using three-dimensional diagrams and two-dimensional contour plots (isolines). These representations were generated from the estimated polynomial equation, with variables restricted to the original experimental domain to ensure the reliability of the predictions.

2.6 Computational environment and statistical tools

All statistical modeling and data processing were conducted using the Python language (version 3.10). For the execution of multiple linear regression via OLS, the "*statsmodels*" library was used. Matrix algebra operations and numerical calculations were performed with the support of the "*numpy*" and "*scipy*" libraries, respectively, while the graphical representations were generated using the "*matplotlib*" library.

REMUNOM
ISSN 2178-6925

Received: 13/01/2026 - **Accepted:** 23/02/2026
Vol: 02.03
DOI: 10.66104/0tq2s573
Pages: 1-22

3. Results and discussion

3.1 Model fitting

The coded quadratic model fitted for the PC1 score presented $R^2 = 0.8134$, adjusted $R^2 = 0.7746$, and overall significance ($p < 0.001$), indicating high explanatory capacity and statistical adequacy. These results demonstrate that the variables working pressure and area per emitter, including their quadratic terms, robustly explain most of the integrated variability of the hydraulic performance synthesized in PC1. The significance of the quadratic terms observed in Table 4 indicates non-linear behavior in the distribution uniformity response relative to the pressure and spacing of the emitters, justifying the adoption of a second-order polynomial model to represent the phenomenon. A predominance of the linear effect associated with the area per emitter (A_c) is observed, followed by the quadratic terms, confirming the greater sensitivity of the integrated uniformity to the spatial variation of the system (Figure 1).

Table 4 - Estimates of the second-order polynomial model coefficients and fit indicators for the PC1 response variable.

Term	Coefficient	Standard Error	t	p-value
Intercept	-0.1151	0.2029	-0.5674	0.5757
P_c	0.1354	0.1440	0.9409	0.3562
A_c	-1.2363	0.1410	-8.7703	<0.001
P_c^2	-0.8133	0.2239	-3.6322	0.0013
A_c^2	0.9540	0.2496	3.8227	<0.001
$P_c A_c$	-0.3212	0.1984	-1.6188	0.1185

P_c: coded value of the operating pressure; A_c: coded value of the area per emitter.
Source: Authors (2026).

REMUNOM
ISSN 2178-6925

Received: 13/01/2026 - **Accepted:** 23/02/2026
Vol: 02.03
DOI: 10.66104/0tq2s573
Pages: 1-22

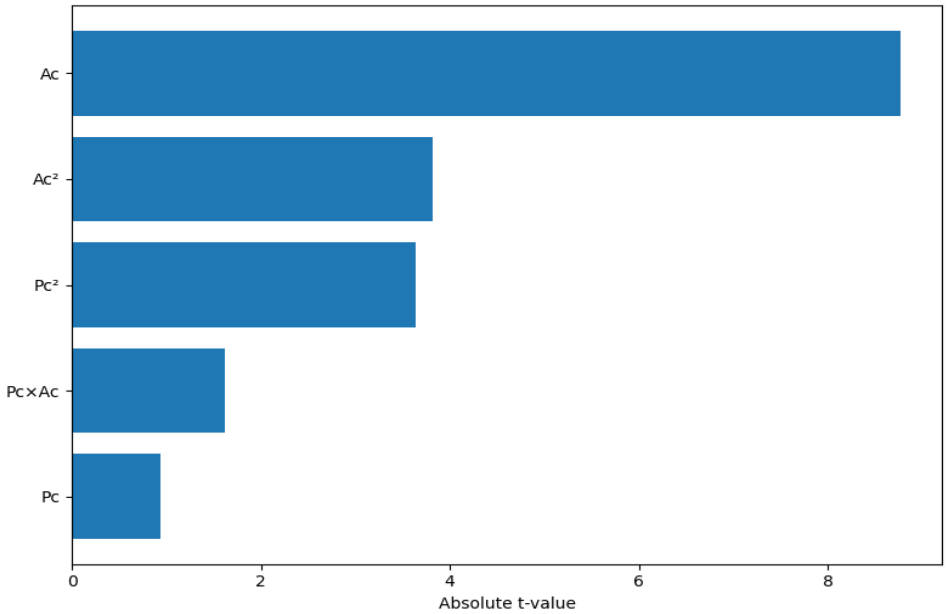

Figure 1 - Pareto chart of standardized effects for the PC1 response surface model. Source: Authors (2026).

The coded quadratic model fitted for PC1 was expressed according to Eq. 5.

$$PC1 = -0{,}1151 + 0{,}1354P_c - 1{,}2363A_c - 0{,}8133P_c^2 + 0{,}9540A_c^2 - 0{,}3212P_cA_c \quad (5)$$

Where: PC1 = value of the first principal component (response variable); P_c: coded value of the operating pressure; A_c: coded value of the area per emitter.

Similar results have been reported in recent experimental studies showing that water application uniformity varies significantly with operating pressure and the spacing of application points: studies with impact sprinklers observed that uniformity measured by coefficients such as CUC and DU tends to decrease as spacing increases, especially under low operating pressures, highlighting the combined influence of these factors on water distribution (Chen et al. 2024).

Furthermore, recent hydraulic analyses indicate that, in sprinkler irrigation systems, water distribution is strongly impacted by arrangement geometry and operating conditions, such as nozzle diameter, inlet pressure, and spacing—all

REMUNOM
ISSN 2178-6925

Received: 13/01/2026 - **Accepted:** 23/02/2026
Vol: 02.03
DOI: 10.66104/0tq2s573
Pages: 1-22

capable of altering application uniformity, especially when combined in mobile or linear systems (Chen et al. 2024).

This non-linear pattern observed in the modeling aligns with agricultural physiology, as the spatial distribution of water directly influences water availability in the soil profile and, consequently, water use efficiency and crop yield. High distribution uniformity has been associated with better water efficiency and crop productivity in field trials, reinforcing the importance of optimizing uniformity as a management strategy (Stambouli et al. 2024).

The negative linear coefficient associated with the area per emitter indicates that larger spacings tend to reduce the system's integrated uniformity, resulting in lower predicted PC1 values. This result agrees with empirical findings where applied water uniformity decreases as the spacing between sprinklers increases, corroborating the role of spatial arrangement in distribution efficiency (Stambouli et al. 2024).

The statistical non-significance of the interaction term P_c x A_c in the model can be associated with the predominance of the main effects of each factor within the experimental range, but it does not exclude the possibility of complementary variations in operating conditions outside the tested limits. Although the interaction term P_c x A_c did not show statistical significance at the 5% level, it was maintained in the model based on the hierarchical principle of Response Surface Methodology, ensuring the preservation of the full polynomial structure and the adequate geometric representation of the fitted surface.

3.2 Model comparison and predictive validation

Model comparison based on information criteria indicated that the full quadratic model, including the interaction term, presented lower AIC (73.57) and BIC (81.98) values compared to the reduced model without interaction (AIC = 77.31; BIC = 84.32) (Table 5). Although the interaction coefficient was not individually significant in the initial regression table, the partial F-test comparing nested models revealed statistical significance ($F = 5.06$; $p = 0.034$), indicating that the removal of the interaction term leads to a significant loss of explanatory capacity.

REMUNOM
ISSN 2178-6925

Received: 13/01/2026 - **Accepted:** 23/02/2026
Vol: 02.03
DOI: 10.66104/0tq2s573
Pages: 1-22

Table 5 – Information criteria (AIC and BIC) and determination coefficients (R^2) for complete and reduced response surface models.

Model	AIC	BIC	R^2
Full (with interaction)	73.57	81.98	0.7593
Reduced (without interaction)	77.31	84.32	0.7085

The stationary point obtained from the nullification of the first-order partial derivatives of Equation 5 was located at P_c = −0.18 and A_c = 0.34 in coded units, corresponding to approximately 1.46 bar and 31.15 m² per emitter in real scale. The predicted PC1 value at this coordinate was −0.51.

Eigenvalue analysis of the Hessian matrix revealed opposite signs, characterizing the stationary point as a saddle point. From a strict mathematical perspective, this indicates that the response surface does not present an internal absolute maximum or minimum within the coded domain.

However, in practical hydraulic optimization, the relevant criterion is not necessarily the mathematical extremum of the fitted response surface, but the maximum predicted response within the bounded experimental region. When the response surface is evaluated under the constraints of the experimental domain (0.5 - 2.5 bar; 9 - 36 m² per emitter), the highest predicted PC1 value (≈ 2.10) occurs at the boundary condition corresponding to pressures near 1.5 bar combined with the smallest tested area (9 m² per emitter).

Therefore, it is essential to distinguish between: (i) the mathematical stationary point, which is a saddle point and does not represent optimal performance; and (ii) the operational optimum within the experimental constraints, located at the boundary region associated with maximum hydraulic overlap.

This distinction resolves the apparent contradiction between the absence of an internal extremum and the identification of a recommended operating range. The model does not indicate a global maximum in the continuous mathematical space, but it does identify the most favorable region within the physically tested conditions.

Based on the bounded experimental evaluation, an operational

REMUNOM
ISSN 2178-6925

Received: 13/01/2026 - **Accepted:** 23/02/2026
Vol: 02.03
DOI: 10.66104/0tq2s573
Pages: 1-22

recommendation can be established for pressures between 1.4 and 1.8 bar combined with areas per emitter equal to or smaller than 12 m². Within this region, predicted PC1 values remain above 1.5, indicating superior integrated hydraulic performance. This recommendation refers explicitly to the experimental domain investigated and should not be interpreted as a universal optimum beyond the studied conditions.

3.3 Statistical model validation

The adequacy of the fitted polynomial model was evaluated through graphical analysis of the residuals, considering their distribution relative to the fitted values and their adherence to normality. Figure 2 shows an approximately random dispersion of the residuals around zero, with no apparent systematic trend or structural pattern, indicating an absence of heteroscedasticity and unmodeled effects.

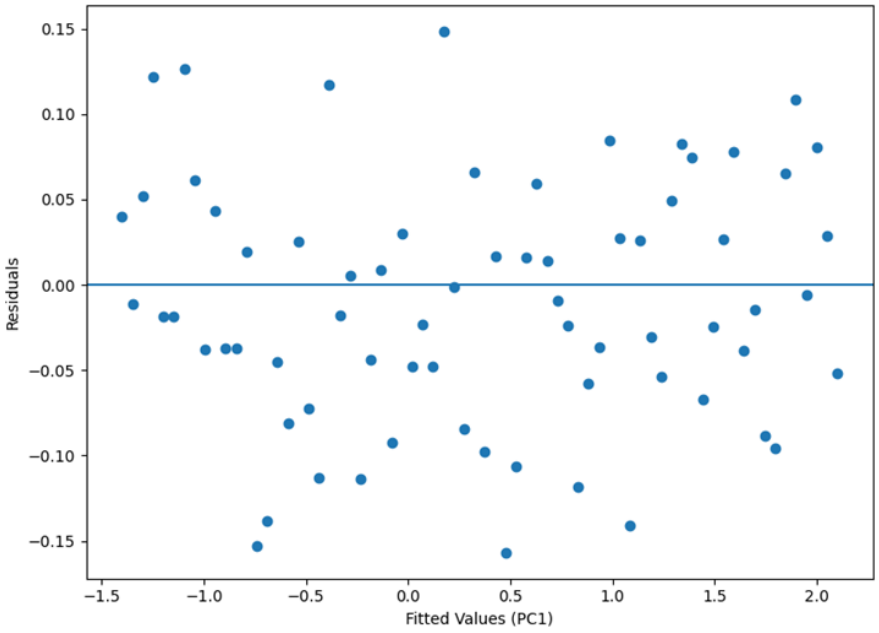

Figure 2 - Residuals as a function of the fitted values of the second-order polynomial model for PC1. Source: Authors (2026).

The Q–Q plot (Figure 3) demonstrates a satisfactory alignment of the points with the theoretical line, suggesting an approximate adherence of the errors to a

REMUNOM
ISSN 2178-6925
Received: 13/01/2026 - **Accepted:** 23/02/2026
Vol: 02.03
DOI: 10.66104/0tq2s573
Pages: 1-22

normal distribution. Taken together, the results indicate that the regression assumptions were met, corroborating the inferential validity of the fitted model.

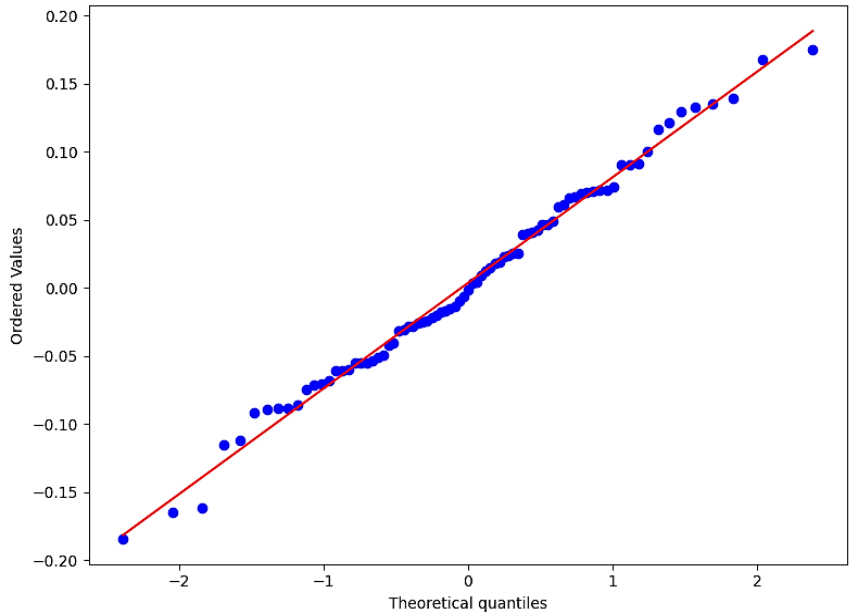

Figure 3 - Q–Q plot of the residuals for the fitted PC1 model. Source: Authors (2026).

The residual analysis indicated an approximately normal distribution as evaluated by graphical inspection of the Q–Q plots (Figure 3) and residuals versus fitted values (Figure 2), along with an absence of structural patterns and homoscedasticity, confirming the adequacy of the fitted polynomial model.

The resulting root mean square error (RMSE) was 0.811, indicating satisfactory predictive stability relative to the observed variability of PC1. Considering that PC1 ranged from approximately −1.71 to 2.12, the RMSE value represents moderate prediction dispersion relative to total variability. This additional validation supports the internal consistency and generalization capacity of the fitted response surface model.

3.4 Response surface analysis

The integrated analysis of the three-dimensional surface and the contour map highlights that the hydraulic performance synthesized by PC1 shows greater

REMUNOM
ISSN 2178-6925

Received: 13/01/2026 - **Accepted:** 23/02/2026
Vol: 02.03
DOI: 10.66104/0tq2s573
Pages: 1-22

sensitivity to the variation in area per emitter than to pressure alone (Figures 4 and 5).

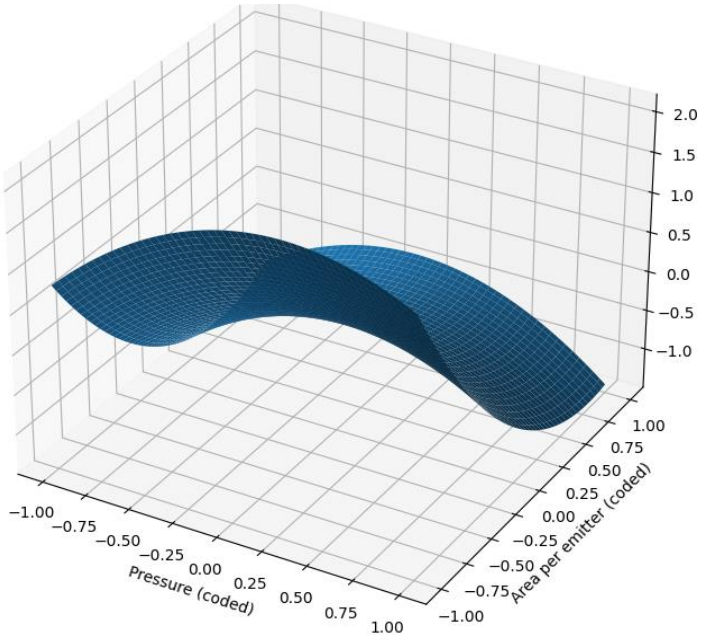

Figure 4 - Response surface for the first principal component score (PC1) as a function of operating pressure (P_c) and area per emitter (A_c) in coded levels. Source: Authors (2026).

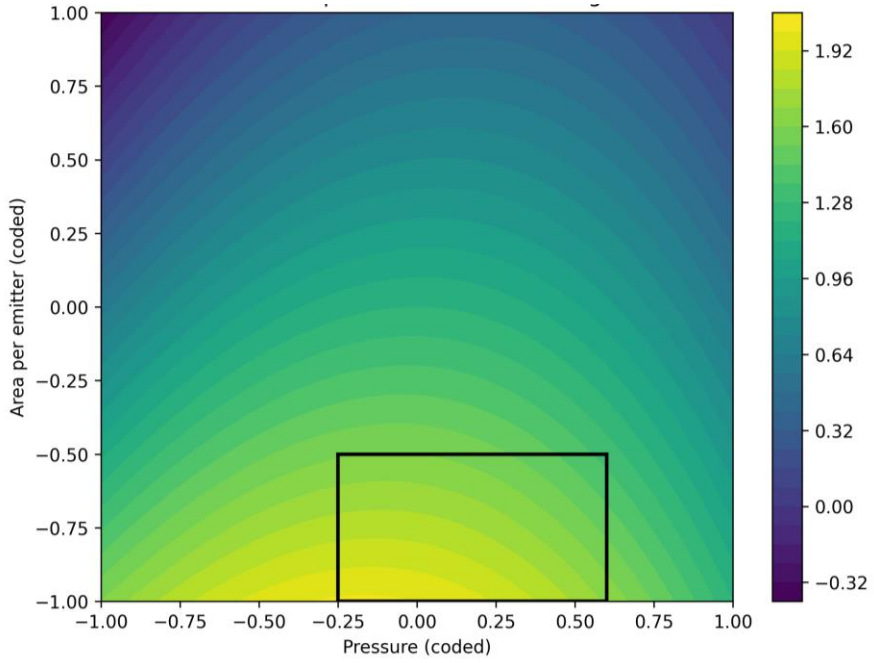

Figure 5 - Contour map of the response surface with the delimitation of the recommended operating region. Source: Authors (2026).

REMUNOM
ISSN 2178-6925

Received: 13/01/2026 - **Accepted:** 23/02/2026
Vol: 02.03
DOI: 10.66104/0tq2s573
Pages: 1-22

The steeper slope along the axis corresponding to spacing confirms that changes in the spatial arrangement exert a more significant impact on the system's integrated uniformity, a behavior widely reported in the literature (Zhu et al. 2022).

Additionally, the significant curvature observed in the pressure direction indicates the existence of an intermediate operating range associated with the highest predicted values of PC1 (Figure 4). In Figure 5, the delimited region corresponds to the recommended operating range, associated with the highest estimated values of integrated uniformity within the experimental domain. Pressures below the optimal range tend to compromise the reach and overlap of the jets, while high pressures may intensify losses due to atomization, drift, and instability in droplet distribution.

These behaviors are compatible with experimental findings demonstrating that pressure loss influences not only uniformity coefficients but also the application rate and jet velocity, which contribute to the formation of non-linear surfaces in response to changes in pressure and spacing (Zhu et al. 2024).

The ellipsoidal configuration of the isolines in the contour map confirms the non-linear nature of the response, typical of second-order polynomial models applied to multivariate hydraulic systems. Studies based on numerical modeling and harmonic analysis of water distribution have also reported similar curvatures resulting from the interaction between geometric and operational parameters (Chen et al., 2024).

Taken together, these findings indicate that system performance depends not only on the isolated adjustment of pressure or spacing but on the harmonization between spatial configuration and hydraulic regime. The obtained response surface, therefore, provides a consistent quantitative basis for technical system optimization, indicating that the maximization of hydraulic performance represented by PC1 is favored by smaller areas per emitter associated with intermediate pressures near 1.5 bar within the evaluated experimental range.

Emerging approaches have explored the use of spectral data obtained by remotely piloted aircraft (RPAs) to map irrigation uniformity in real-time, offering a

REMUNOM
ISSN 2178-6925

Received: 13/01/2026 - **Accepted:** 23/02/2026
Vol: 02.03
DOI: 10.66104/0tq2s573
Pages: 1-22

complementary perspective to traditional analyses based on coefficients and response surfaces (Santana et al. 2025).

The proposed model is valid within the evaluated experimental domain and for the hydraulic configuration of the Hadar 7110 microsprinkler. It should be noted that spacing configurations were obtained through computational simulation using the quadrant overlap method, whereas pressures were measured under field conditions. This methodological distinction implies that spacing assumes idealized overlap and negligible wind interference.

Environmental factors such as wind drift, terrain variability, and emitter manufacturing differences may alter water distribution patterns and modify the response surface geometry. Therefore, the operational recommendations apply strictly to the tested pressure (0.5–2.5 bar) and spacing (9–36 m² per emitter) ranges. Extrapolation beyond these limits or to different emitter models should be undertaken with caution.

Future studies incorporating dynamic wind conditions and full-field validation may further expand the model's external applicability.

4. Conclusions

The quadratic model fitted for the PC1 score demonstrated statistical robustness ($R^2 = 0.8134$; $p < 0.001$), confirming that working pressure and area per emitter satisfactorily describe the integrated hydraulic performance. The significance of second-order terms evidences the nonlinear behavior and curvature of the response surface.

Canonical analysis identified a stationary saddle point (1.46 bar and 31.15 m² per emitter), indicating the absence of an internal optimum within the experimental domain. Superior performance (PC1 ≈ 2.10) was observed along the experimental boundaries, particularly under pressures near 1.5 bar combined with the smallest tested area per emitter (9 m²).

Integrated uniformity proved to be more sensitive to spatial configuration than to isolated pressure variation. To achieve superior hydraulic performance within the evaluated domain, operation is recommended at pressures between 1.4 and 1.8 bar

REMUNOM
ISSN 2178-6925

Received: 13/01/2026 - **Accepted:** 23/02/2026
Vol: 02.03
DOI: 10.66104/0tq2s573
Pages: 1-22

associated with emitter areas equal to or less than 12 m². Response surface modeling demonstrated effectiveness in harmonizing operating pressure and spatial arrangement in micro-sprinkler systems.

References

ABD EL-WAHED, M. H.; MEDICI, M.; LORENZINI, G. Sprinkler irrigation uniformity: impact on crop yield and water use efficiency. Journal of Engineering Thermophysics, v. 25, n. 1, p. 117-125, 2016. DOI: 10.1134/S1810232816010112.

AMARAL, A. M.; FARIAS, A. M.; SANTOS, M. Â. C. M.; ANORATO, L. R. et al. Análise de componentes principais aplicada à uniformidade de irrigação por microaspersão. In: VILA VERDE, D. S. et al. Produção Vegetal na Agronomia: abordagens e aplicações. 2. ed. Teresina-PI: Wissen, 2025. p. 214-222. DOI: 10.52832/wed.169.980.

ANDRADE, L. M.; PACHECO, J. C.; COSTA, G. L. L.; ALENCAR, C. A. B.; CUNHA, F. F. Uniformity of water distribution by a sprinkler irrigation system on a soccer field. Bioscience Journal, v. 38, e38012, 2022. DOI: 10.14393/BJ-v38n0a2022-57028.

ASSOCIAÇÃO BRASILEIRA DE NORMAS TÉCNICAS (ABNT). NBR 15084: Sistemas de irrigação localizada - Microaspersores - Ensaios de desempenho. Rio de Janeiro: ABNT, 2021.

BERNARDO, S.; MANTOVANI, E. C.; SILVA, D. D.; SOARES, A. A. Manual de Irrigação. 9. ed. Viçosa: Ed. UFV, 2019. 545 p.

BOX, G. E. P.; WILSON, K. B. On the Experimental Attainment of Optimum Conditions. Journal of the Royal Statistical Society: Series B, v. 13, n. 1, p. 1-45, 1951. DOI: 10.1111/j.2517-6161.1951.tb00067.x.

CHEN, X.; CHEN, R.; WANG, J.; LI, H.; ZHANG, W. Evaluation of water distribution and uniformity of sprinkler irrigation based on harmonic analysis and finite element method. Biosystems Engineering, v. 248, p. 308-320, 2024. DOI: 10.1016/j.biosystemseng.2024.11.010.

FARIAS, A. M.; COSTA, L. A. B.; BRITO, A. F. C.; OLIVEIRA, L. A.; AMARAL, A. M.; SANTOS, M. Â. C. M. Uniformidade de distribuição do microaspersor Hadar 7110 operando sob variabilidade de pressão de serviço e espaçamento em condições de campo. Research, Society and Development, v. 13, n. 5, e11613545896, 2024. DOI: 10.33448/rsd-v13i5.45896.

REMUNOM
ISSN 2178-6925

Received: 13/01/2026 - **Accepted:** 23/02/2026
Vol: 02.03
DOI: 10.66104/0tq2s573
Pages: 1-22

JOLLIFFE, I. T.; CADIMA, J. Principal component analysis: a review and recent developments. Philosophical Transactions of the Royal Society A, v. 374, 2016. DOI: 10.1098/rsta.2015.0202.

KHURI, A. I.; CORNELL, J. A. Response Surfaces: Designs and Analyses. 2. ed. New York: Marcel Dekker, 1996. DOI: 10.1201/9780203740774.

MOURA NETO, J. M. de; NASCIMENTO, A. A. do; SILVA, I. O. da; OLIVEIRA, C. E. de; SILVA, A. R. A. da; FERNANDES, C. N. V. Coeficientes de uniformidade na irrigação por aspersão convencional em área de pastagem cultivada. Irriga, v. 29, p. 162-168, 2024. DOI: 10.15809/irriga.2024v29p162-168.

NAIR, A. T.; MAKWANA, A. R.; AHAMMED, M. M. The use of response surface methodology for modelling and analysis of water and wastewater treatment processes: a review. Water Science & Technology, v. 69, n. 3, p. 464-478, 2014. DOI: 10.2166/wst.2013.733.

OLIVEIRA, J. A. M.; OLIVEIRA, C. M. M. Balanço hídrico climatológico e classificação climática para o município de Arinos - MG. Revista Brasileira de Agricultura Irrigada, v. 12, n. 6, p. 3021-3027, 2018. DOI: 10.7127/rbai.v12n600901.

PAULINO, M. A. de O.; FIGUEIREDO, F. P. de; FERNANDES, R. C.; MAIA, J. T. L. S.; GUILHERME, D. O.; ALMEIDA, A. C. S. Avaliação da uniformidade e eficiência de aplicação de água em sistemas de irrigação por aspersão convencional. Revista Brasileira de Agricultura Irrigada, v. 3, n. 2, p. 48-54, 2009. DOI: 10.7127/rbai.v3n200011.

PRADO, G.; COELHO, T. B. B.; TINOS, A. C.; MAHL, D.; BORTOLETTO, E. C. Distribuição de água de microaspersor para diferentes condições operacionais. Irriga, v. 26, n. 4, p. 867-883, 2021. DOI: 10.15809/irriga.2021v26n4p867-883.

RODRIGUES, L. G.; NERY, A. R.; SOUSA, F. R. R.; RODRIGUES, L. N. Coeficientes de uniformidade em aspersores de baixa vazão com diferentes arranjos e altura da haste. Revista Verde de Agroecologia e Desenvolvimento Sustentável, v. 14, n. 2, p. 170-180, 2019. DOI: 10.18378/rvads.v14i2.6335.

SANTANA, L. S.; OLIVEIRA, R. T.; COSTA, F. B.; SILVA, M. A.; PEREIRA, G. H.; LIMA, J. R. Analysis of sprinkler irrigation uniformity via multispectral data from RPAs. Eng, v. 6, n. 10, p. 268, 2025. DOI: 10.3390/eng6100268.

STAMBOULI, T.; FOUILLEN, A.; LADEIRA-ANDRADE, A.; DEJEAN, C.; SINFORT, C.; SOTO-GARCIA, M. Analysis of droplet size and velocity distribution of a new prototype of impact sprinkler. Agricultural Water Management, v. 284, p. 108342, 2023. DOI: 10.1016/j.agwat.2023.108342.

REMUNOM
ISSN 2178-6925

Received: 13/01/2026 - **Accepted:** 23/02/2026
Vol: 02.03
DOI: 10.66104/0tq2s573
Pages: 1-22

ZHU, X.; YUAN, S.; LI, T.; LIU, J.; JIANG, Z. Characteristics of rotary sprinkler water distribution under dynamic water pressure. Horticulturae, v. 8, n. 9, p. 804, 2022. DOI: 10.3390/horticulturae8090804.

ZHU, X.; FORDJOUR, A.; DWOMOH, F. A.; LEWBALLAH, J. K.; OFOSU, S. A.; LIU, J.; DAI, X.; OTENG, J. Experimental study on the effects of pressure loss on uniformity, application rate and velocity on different working conditions using the dynamic fluidic sprinkler. Heliyon, v. 10, p. e27140, 2024. DOI: 10.1016/j.heliyon.2024.e27140.